CONCLUSION

Experimental data obtained on samples of n-type $CdAs_2$ have been fitted to a simple energy-band model consisting of either a single conduction-band minimum at $k=0$ or two minima located at equivalent points along k_z. This is in agreement with cyclotron resonance observations. Values of the anisotropy constant $K=\tau_{\parallel}m_{\perp}/\tau_{\perp}m_{\parallel}$ were obtained from Hall and resistivity data and indicate that $\tau_{\parallel}/\tau_{\perp}$ is approximately unity above 250°K.

ACKNOWLEDGMENTS

The author wishes to thank Dr. J. F. Woods and Dr. W. J. Turner for many helpful discussions during the course of this work and Dr. R. W. Keyes for his valuable comments during the preparation of the manuscript. He would also like to thank V. J. Silvestri for the preparation and cutting of the samples and to acknowledge the assistance of J. Keller and E. F. Gorey in making the electrical measurements, N. R. Stemple for x-ray orientation of the crystals, and D. P. Cameron for the spectrographic data of Table I.

PHYSICAL REVIEW VOLUME 122, NUMBER 2 APRIL 15, 1961

Nuclear Quadrupole Resonance in an Antiferromagnet

J. C. BURGIEL,*† V. JACCARINO, AND A. L. SCHAWLOW
Bell Telephone Laboratories, Murray Hill, New Jersey

(Received December 13, 1960)

Nuclear quadrupole resonance techniques have been used to investigate magnetic interactions in the bromates and iodates of certain $3d$ transition metal ions. In particular, for $Ni(IO_3)_2\cdot 2H_2O$ there is an abrupt disappearance of the $I^{127}(\pm 3/2 \leftrightarrow \pm 1/2)$ transition at 3.08°K; at lower temperatures there is a large, temperature-dependent splitting. This behavior is attributed to the combined effects of an antiferromagnetic ordering of the Ni^{++} electron spins and a hfs interaction of the nonlocalized Ni^{++} spin magnetization with the I^{127} nuclear magnetic moment. Measurements of the pure quadrupole transition frequencies above, and of their temperature-dependent splittings below, the Néel temperature yield the quadrupole coupling constant, the asymmetry of the electric field gradient (EFG) tensor, the magnitude and orientation of the internal magnetic field relative to the principal axes of the EFG tensor, and the sublattice magnetization as a function of temperature. Qualitative experiments at 1.3°K indicate $T_1^{127}\ll 100$ sec and $T_2^{127}\sim 10^{-6}$ sec. Measurements of the rf and dc magnetic susceptibility have been made and are consistent with these conclusions and, in addition, indicate the sudden onset of a spontaneous ferromagnetic moment as the temperature is lowered below T_n. A possible isotope effect on the T_n of $Ni(IO_3)\cdot 2H_2O$ was looked for but none was found. Cupric iodate and the bromates give no evidence of magnetic ordering above 1.3°K.

INTRODUCTION

WE present in the following the results of observations of nuclear quadrupole resonance in an antiferromagnet.[1] Since this constitutes the first such observation, we briefly review nuclear resonance phenomena in antiferromagnets.

In recent years the techniques of nuclear magnetic resonance (NMR) have been successfully applied to the study of local fields in magnetic solids both in the paramagnetic and ordered states. If, in addition, a nucleus possesses an electric quadrupole moment Q, and is subject to an electric field gradient (EFG), resonances may be observable without an external magnetic field, either in single crystals or in polycrystalline samples. These so called "pure quadrupole resonances" we denote by NQR. Aside from the experimental convenience, observation of the quadrupole transitions permits a comparison of the directions of the EFG tensor and internal magnetic field in an ordered magnetic material.

Before discussing the effects that result from combined nuclear magnetic moment and nuclear electric quadrupole moment interactions, it is perhaps instructive to briefly classify the nuclei according to their electronic environments and their possible electric and magnetic interactions. (We restrict our discussion to insulating magnetic solids.)

Magnetic interactions. (1) Nuclei of paramagnetic ions (e.g., Co^{59} in CoF_2).[2] The nucleus is immersed in large hyperfine fields arising from the magnetic electrons of *its own* ion in addition to the dipolar fields of all other magnetic ions.

(2) Nuclei of nominally diamagnetic ions (e.g., F^{19} in CoF_2).[3] If an appreciable overlap exists between the

* Submitted in partial fulfillment of the requirements for the degree of Master of Science, Department of Electrical Engineering (1959), Massachusetts Institute of Technology, Cambridge, Massachusetts.

† Present address: Department of Physics, Massachusetts Institute of Technology, Cambridge, Massachusetts.

[1] A preliminary report of this work was given at the November, 1959 American Physical Society Meeting [J. C. Burgiel, V. Jaccarino, and A. L. Schawlow, Bull. Am. Phys. Soc. 4, 424 (1959)].

[2] V. Jaccarino, Phys. Rev. Letters 2, 163 (1959).

[3] V. Jaccarino, R. G. Shulman, and J. W. Stout, Phys. Rev. 106, 602 (1957).

wave functions of the diamagnetic ion and a neighboring paramagnetic ion, then a spatial redistribution of the paramagnetic electrons will induce a partial paramagnetic character in the overlapping closed-shell electrons of the diamagnetic ion. Then, as in case (1), hyperfine interactions with the partial paramagnetism of its own electrons are possible.[4–8]

(3) Nuclei of truly diamagnetic ions (e.g., H^1 in $CuCl_2\cdot 2H_2O$).[9] The nucleus is subjected only to the dipolar fields of the paramagnetic ions.

Electric interactions. Nuclei with $I\geq 1$ in lattice sites whose point symmetry is sufficiently low that the components of the electric field gradient (EFG) tensor do not vanish may have an electric quadrupole interaction e^2qQ.[10] We may classify these interactions according to their origin and magnitude as follows:

(1) The EFG results principally from the electrons of their own ions (e.g., Co^{59} in CoF_2): $e^2qQ\lesssim\mu H$.

(2) The EFG results from the charges of neighboring ions and relatively weak covalent bonding to these ions (e.g., Cl^{35} in $TiCl_3$ [11]): $e^2qQ\gtrsim\mu H$.

(3) Nuclei for which the EFG results from strong covalent bonding (I^{127} in IO_3^- as in this work[12]): $e^2qQ\gg\mu H$.

Experimentally, for nuclei in the last two categories it is possible to study NQR in the absence of external magnetic fields both in the paramagnetic and ordered states.[13] NQR for the case in which $e^2qQ\gg\mu H$ in the ordered state and for which indirect hyperfine interactions would exist is of particular interest and was the prime motivation for the present work.

In order to study the effects of magnetic ordering on NQR, a search was made for an antiferromagnet in which NQR could be observed. The bromates of certain $3d$ group transition metals were investigated first; their quadrupole spectra gave no indications of magnetic ordering. For reasons described below, attention was turned toward the iodates of the same metals. $Ni(IO_3)_2\cdot 2H_2O$ proved to be the compound sought for and became the first antiferromagnet to be discovered from observations of NQR. From the detected quadrupole spectra, the direction of the spin magnetization relative to the EFG tensor was determined. From the temperature dependence of the frequencies below the Néel temperature T_n, the temperature dependence of the sublattice magnetization was obtained. Measurements of the rf and dc magnetic susceptibility confirmed these results and indicated the presence of a spontaneous ferromagnetic moment that results from slight cocking of the antiferromagnetic sublattices.

ELEMENTARY THEORY

The Hamiltonian for the Zeeman effect of quadrupole spectra may be written as

$$\mathcal{H}=\mathbf{I}\cdot\mathbf{K}\cdot\mathbf{I}-\gamma\mathbf{I}\cdot\mathbf{H}, \tag{1}$$

where $\mathbf{K}$ is a second rank tensor describing the interaction of the nuclear electric quadrupole moment with the gradient of the surrounding electric field and $\gamma=\mu/I$. With the principal coordinate system (x,y,z) of the EFG tensor defined in the usual way, Eq. (1) may be written as

$$\mathcal{H}=3A[I_z^2-\tfrac{1}{3}I(I+1)]+\eta A[I_x^2-I_y^2]-\gamma\mathbf{I}\cdot\mathbf{H}, \tag{2}$$

where $A=e^2qQ/[4I(2I-1)]$ in which $eq=\partial^2V/\partial z^2$ and Q is the electric quadrupole moment of the nucleus, and where $\eta=(\partial^2V/\partial x^2-\partial^2V/\partial y^2)/(\partial^2V/\partial z^2)$ is the asymmetry parameter. It is interesting to note the formal similarity between the quadrupole Hamiltonian and the spin Hamiltonian that describes the interaction of a magnetic ion with the external field and the electrostatic fields in a crystal.[14] The latter, to terms quadratic in the spin operator, may be written as[15]

$$\begin{aligned}\mathcal{H}&=\mathbf{S}\cdot\mathbf{D}\cdot\mathbf{S}+g\beta\mathbf{S}\cdot\mathbf{H}\\&=D[S_z^2-\tfrac{1}{3}S(S+1)]+E[S_x^2-S_y^2]+g\beta\mathbf{S}\cdot\mathbf{H},\end{aligned} \tag{3}$$

where $\mathbf{D}$ is the crystal field tensor. This equivalence is a consequence of the identity of the transformation properties of the respective tensors under rotation and hence, by the Wigner-Eckart theorem, the corresponding Hamiltonians have matrix elements with the same m dependence. (The formal equivalence of the electron spin Hamiltonian, including only terms quadratic in $\mathbf{S}$, with the nuclear electric quadrupole Hamiltonian is exact but cannot be extended to higher order terms.)

The recognition of the equivalence of (2) and (3) is useful in our case because procedures for diagonalizing the spin Hamiltonian exist and have been extensively employed by M. Peter and B. B. Cetlin. The relation

[4] R. G. Shulman and V. Jaccarino, Phys. Rev. **108**, 1219 (1957).
[5] A. Mukherji and T. P. Das, Phys. Rev. **111**, 1479 (1958).
[6] W. Marshall, Bull. Am. Phys. Soc. **4**, 142 (1959).
[7] F. Keffer, T. Oguchi, W. O'Sullivan, and J. Yamishita, Phys. Rev. **115**, 1553 (1959).
[8] A. M. Clogston, J. P. Gordon, V. Jaccarino, M. Peter, and L. R. Walker, Phys. Rev. **117**, 1222 (1960).
[9] N. J. Poulis, G. E. G. Hardeman, and B. Bolger, Physica **18**, 429 (1952).
[10] This restriction on symmetry need not be applied to the rare earth ions in cubic crystals because the angular momentum of the magnetic electrons is not quenched. The $4f$ ions and their nuclei enjoy all electrostatic interactions that the free atom has in this case.
[11] R. G. Barnes and S. L. Siegel, Phys. Rev. Letters. **3**, 462 (1959).
[12] This is the usual case for NQR and an extensive literature exists. See T. P. Das and E. L. Hahn, in *Solid-State Physics*, edited by F. Seitz and D. Turnbull (Academic Press Inc., New York, 1958), Suppl. 1.
[13] Restrictions on the observation of a nuclear resonance in a magnetic material may exist either due to a short nuclear-spin lattice relaxation time T_1 or because of line-broadening mechanisms.
[14] W. Low, in *Solid-State Physics*, edited by F. Seitz and D. Turnbull (Academic Press Inc., New York, 1960), Suppl. 2.
[15] The change in sign in the last term arises because $\beta=\mu/S$ is conventionally given as a positive number whereas it is, of course, negative. For simplicity we consider g as being a scalar quantity.

between the parameters to be determined and the measured quantities is, by the nature of the experimental conditions, different in the two cases, however. In electron paramagnetic resonance studies a known field is usually applied externally in a given direction with respect to the crystal axes and, from the angular dependence of the observed level splittings as a function of field and frequency, the parameters D and E can be determined. In contrast to this, our observations in the NQR case yield partial information in each of the two magnetic states: (1) the paramagnetic state, in which, in expression (2), $H_{\text{int}}=0$ and in which, if $I>\frac{3}{2}$, A and η may be determined without the aid of an external magnetic field; (2) the ordered state, in which an internal field arises from spin ordering and is an unknown function of temperature. Both the magnitude and direction of the field relative to the principal axes of the EFG tensor at the site of the resonant nucleus must be determined. To extract the desired information our computational problem involved only rearranging the computer programming procedure to obtain the requisite parameters.

EXPERIMENTAL PROCEDURE AND RESULTS

The high-frequency NQR transitions were observed with a super-regenerative detector[16] in zero external field. In single crystals of the paramagnetic bromates the $(\pm\frac{1}{2}\leftrightarrow\mp\frac{1}{2})$ transitions were observed with a Varian Associates NMR spectrometer and magnet. The resonant coil of the super-regenerative detector was externally mounted, but concentric with the unsilvered tip of a special cryostat which contained the samples. Precise measurements of temperature in the liquid helium range were made using a vapor pressure manometer. Frequency measurements were accomplished using a stable oscillator for frequency markers and a crystal-controlled frequency counter.

Paramagnetic bromates. Initially the NQR of $Br^{79,81}$ in the cubic bromate-hexahydrates of divalent Co, Ni, and Cu were investigated as a function of temperature because their spectra had previously been studied at 200°K and 300°K.[17] However, no ordering was observed in any of these salts above 1.3°K, the lowest temperature achievable in our cryostat. The structure of these bromates[18] is such that molecules of the water of hydration form an octahedron about each paramagnetic ion. As a consequence of this, a negligible overlap of the wavefunctions of the magnetic ion and the bromate radical exists. A superexchange interaction between two paramagnetic ions would have to involve the polarization of at least *two* intervening water molecules. It is reasonable to expect the magnitude of such a "dilute" interaction to be considerably less than 1°K. Moreover, we were unable to find a bromate structure in which the bromate radical is the intervening anion between two paramagnetic cations. Our attention turned towards crystals which would appear to be more magnetically concentrated. In particular, it would seem desirable to have two magnetic ions interact through, say, a single ClO_3^- or IO_3^- radical. From the known range of frequencies for Cl and I nuclear quadrupole resonances[12] in the latter two radicals and the experimental apparatus immediately available for search purposes, it was decided to investigate magnetic iodate crystals.

$Ni(IO_3)_2\cdot 2H_2O$

Although at the outset of our research little was known about the crystal structure of $Ni(IO_3)_2\cdot 2H_2O$, we decided to investigate the NQR of I^{127} in this compound simply because of the smaller relative concentration of waters of hydration.

The sample was prepared[19] by adding nickel carbonate to iodic acid, redissolving the resulting precipitate, and then slowly boiling away the water. Tiny crystals were produced, the largest of which were less than $\frac{1}{3}$ mm in any dimension. Recently, some preliminary information on the crystal structure has been obtained.[20] This is illustrated, approximately to scale, in Fig. 1. The unit cell is orthorhombic with dimensions (in angstroms) $a=9.18\pm0.05$, $b=12.20\pm0.05$, $c=6.60\pm0.05$. The space group is $D_{2h}^{15}-Pbca$. All iodine atom sites are physically equivalent.

An initial search was made for the $(\pm\frac{3}{2}\leftrightarrow\pm\frac{1}{2})$ transition in the neighborhood of 150 Mc/sec at a tem-

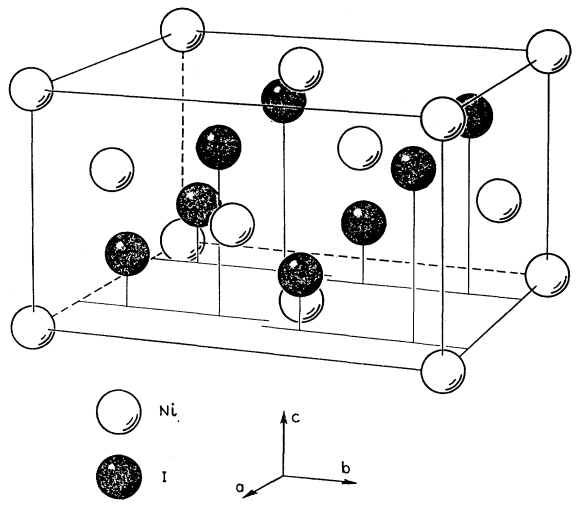

FIG. 1. The positions of the nickel and iodine atoms in β-$Ni(IO_3)_2\cdot 2H_2O$. The crystal is orthorhombic with unit cell dimensions: $a=9.18$, $b=12.20$, $c=6.60$ A. The most probable space group is D_{2h}^{15}-*Pbca* with four formula weights in a unit cell. All iodine atom sites are physically equivalent.

[16] A. L. Schawlow, J. Chem. Phys. **22**, 1211 (1954).
[17] K. Shimomura, T. Kushida, N. Inoue, and Y. Imaeda, J. Chem. Phys. **22**, 1944 (1954).
[18] S. H. Yu and C. A. Beevers, Z. Krist. **95**, 426 (1936).
[19] Nickel iodate exists in three forms: a tetrahydrate and two dihydrates. We are interested in the β-dihydrate. A. Meusser, Ber. deut. chem. Ges. **34**, 2432 (1901).
[20] E. A. Wood (private communication).

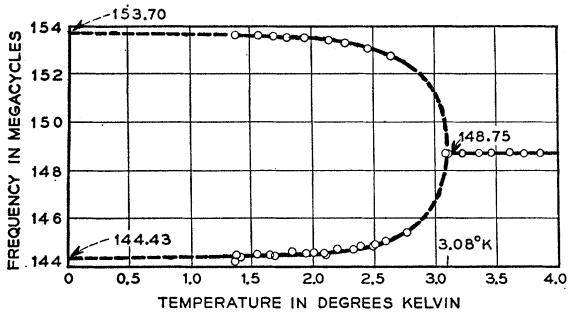

FIG. 2. The frequency of the I^{127} NQR transition $(\pm\frac{3}{2}\leftrightarrow\pm\frac{1}{2})$ in $Ni(IO_3)_2\cdot 2H_2O$ as a function of temperature. The abrupt disappearance of the resonance, as the temperature is lowered, occurs at 3.08°K. The average of the $T=0$ limits for the two branches is 149.065 Mc/sec.

perature of 4.2°K after some elementary considerations[16] concerning the known spectra of other iodate crystals. A resonance that was temperature independent in the immediate vicinity of 4°K and, which remained so between 4°K and 20°K was observed at 148.75 Mc/sec. A peculiar feature of this resonance was noticed. During a period of several weeks following the initial preparation and use of the sample, the resonant frequency increased to about 148.97 Mc/sec. We believe this effect to result from the local annealing that follows intermittent warming and cooling after initial crystal growth at 100°C.

If $\eta=0$ the $(\pm\frac{5}{2}\leftrightarrow\pm\frac{3}{2})$ resonance should occur at twice the frequency of the $(\pm\frac{3}{2}\leftrightarrow\pm\frac{1}{2})$ transition or 297.50 Mc/sec. A resonance was initially found at 296.62 Mc/sec and correspondingly increased to about 297.05 Mc/sec as a function of time. From these two observations η and e^2qQ may be determined from a table prepared by Livingston and Zeldes.[21] The values so obtained (after "annealing") are given in Table I.

As the temperature was lowered, the $(\pm\frac{3}{2}\leftrightarrow\frac{1}{2})$ resonance was observed to disappear abruptly at 3.08°K. Below 2.9°K two resonances were found with the temperature dependence shown in Fig. 2. Between 2.9°K and 3.08°K the resonances are not observable, possibly because of intrinsic line broadening to be expected in the region of T_n or more likely because of the combined effect of slight temperature inhomogeneities in the sample and the strong temperature dependence of the resonant frequency in this region. The $(\pm\frac{5}{2}\leftrightarrow\pm\frac{3}{2})$ resonance changes its effect on the superregenerative detector somewhat (see Fig. 3) due to a small splitting discussed in the caption to Fig. 3 and decreases its frequency by 38±3 kc/sec as the temperature is lowered from 3.08° to 1.3°K. All resonances at 1.3°K are estimated to have a width at half power of approximately 80 kc/sec corresponding to a $T_2^{127}\sim 10^{-6}$ sec. No indication of saturation was found at our maximum rf level (~1 volt). The amplitude of the rf field was empirically determined from the known saturation behavior of the high-frequency NMR of F^{19} in antiferromagnetic MnF_2.[22] In this way an upper limit of $T_1^{127}\ll 100$ sec could be set on the nuclear spin-lattice relaxation time at 1.3°K from the absence of saturation of the $(\pm\frac{3}{2}\leftrightarrow\pm\frac{1}{2})$ transition in $Ni(IO_3)_2\cdot 2H_2O$.

To obtain the internal magnetic field at the I^{127} nucleus at temperatures below T_n the following procedure was employed. The "zero-field" intervals obtained from the paramagnetic state measurements were combined with the observed splittings of the two transitions at a given temperature $T<T_n$ in a first-order perturbation calculation of $H_{\rm int}(T)$. The quadrupole Hamiltonian, expression (2), was then diagonalized exactly for a range of values of $H_{\rm int}$, θ, and φ (the polar and azimuthal angles specifying the direction of $H_{\rm int}$ relative to the principal coordinate system of the EFG tensor) in the neighborhood of the approximate values determined from the perturbation calculation. It is interesting to note that the splitting of the transitions is proportional to the magnetic field to a high degree of accuracy. The nonlinear terms are smaller than the linear terms by a factor $(\mu H_{\rm int}/e^2qQ)^2$. Assuming that e^2qQ and η do not change in the antiferromagnetic region, we obtain on the basis of this information the magnitude, temperature dependence, and direction of $H_{\rm int}$ relative to the principal axes of the EFG tensor. At the site of the I^{127} nucleus $H_{\rm int}(T=0)=3400$ oe. An estimate of the electronic dipolar field gives an approximate value of 800 oe. We presume the difference to have its origin in the indirect hfs interaction of the I^{127} nucleus on the Ni^{2+} spin. Table I summarizes these results.

Though no detailed interpretation concerning the indirect hyperfine interaction between the Ni^{++} spin and the I^{127} nuclear moment will be attempted for the present, a few words concerning the origin of the interaction are perhaps in order. The nearest neighbors of a Ni^{++} ion are an octahedron of O ions, two of which belong to the waters of hydration and the remaining four belong to the (IO_3) radicals.[20] Thus one might think no appreciable overlap of Ni and I wave functions would exist. However, it is to be remembered that the I-O bond is extremely covalent, and the I $5s$ and $5p$ wave functions and O $2s$ and $2p$ wave functions

TABLE I. Results derived from the NQR of I^{127} in the paramagnetic and antiferromagnetic states of $Ni(IO_3)_2\cdot 2H_2O$. θ and φ are, respectively, the polar and azimuthal angles specifying the direction of $H_{\rm int}$ relative to the principal axes of the EFG tensor.

Paramagnetic state	$\eta=0.048$ $(1/h)e^2qQ=990.65$ Mc/sec
Antiferromagnetic state	$H_{\rm int}^{127}(0°K)=3400$ oe $\theta=90°\pm5°$, $\varphi=90°\pm10°$ $T_1\ll 100$ sec, $T_2\sim 10^{-6}$ sec

[21] Livingston and H. Zeldes, Oak Ridge National Laboratory Report ORNL-1913, 1955 (unpublished).

[22] V. Jaccarino and R. G. Shulman, Phys. Rev. **107**, 1196 (1957).

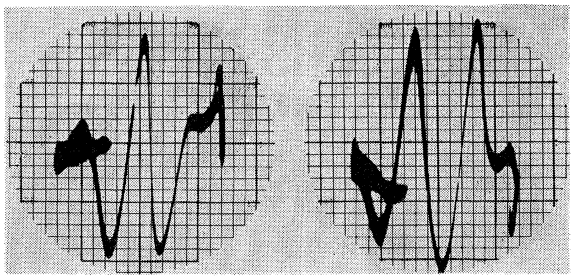

FIG. 3. Photograph of the oscilloscope presentation of the I^{127} NQR transition ($\pm\frac{5}{2} \leftrightarrow \pm\frac{3}{2}$) when (a) $T=4.2°K$ ($T>T_n$) and (b) $T=1.3°K$ ($T<T_n$). Calculations indicate that at 1.3°K all observed lines are actually doublets with a 536 kc/sec splitting. In order to resolve such doublets with a super-regenerative detector, one needs a quench frequency greater than the linewidth and either very much less or very much greater than the splitting. Because the lines are so broad in this case, one must use a quench frequency very much greater than 500 kc/sec. The detector used would not operate with such quench frequencies. The patterns on the oscilloscope were therefore not absorption lines but rather interference patterns of two lines and their images from sidebands of the detector. The frequencies used in the calculations were the frequencies of the centers of symmetry of the patterns. As would be expected, changing the quench frequency changed the pattern but did not shift its center of symmetry.

are therefore strongly admixed. (The large I electric quadrupole interaction is a manifestation of the covalent character of the I-O band and the hybridization of s and p wave functions.) For our purpose this has as a consequence a spatial extension of the I $5s$ and $5p$ orbits to a region that largely includes all of the (IO_3) radical.

The overlap of the $3d$ Ni^{++} wave functions with the spatially extended I $5s$ and $5p$ wave functions is the origin of the magnetic hyperfine interaction at the I^{127} nucleus. There are two contributions to the hyperfine interaction.[5–8] The overlap of the unpaired $3d$ electrons with the paired (diamagnetic) $5s$ and $5p$ electrons produces a partial polarization of s and p electrons with spin direction *parallel* to that of the d electrons. This effect is a consequence of the nonorthogonality of the $3d$ and $5s$ and $5p$ wave functions. There is also a contribution to the polarization of $5s$ and $5p$ electrons which results from electron transfer of I electrons into Ni $3d$ orbits. Since the Ni^{++} $3d$ electrons are Hund's-rule coupled and the d shell is more than half filled, a *parallel* spin polarization is expected in this case as well.

In the paramagnetic state, the thermal average of the spin polarization $\langle S_z\rangle$ is zero in the absence of an external magnetic field. In the antiferromagnetic state $\langle S_z\rangle$ is proportional to the sublattice magnetization. The magnitude of the magnetic field at the iodine nucleus in the antiferromagnetic state is

$$H_T{}^{127}=(A_{\text{mag}}{}^{127}/g\beta)\langle S_z\rangle_T, \tag{4}$$

where $A_{\text{mag}}{}^{127}$ is the effective magnetic hyperfine interaction between the Ni^{++} spin and the I^{127} nuclear moment.[4,22]

A more detailed interpretation of the indirect hyperfine interaction would be possible if single crystals of sufficient size were available for Zeeman studies.

The normalized temperature dependence of H_{int} is given in Fig. 4 along with the magnetization curve calculated from molecular-field theory assuming $S=1$, corresponding to the spin of Ni^{++}. In the temperature range between 2° to 3°K, H_{int} falls off faster than T^6. The lack of agreement between experiment and theory testifies to the inadequacy of the simple molecular-field theory which neglects the effects of large, anisotropic crystal fields. The observed behavior of the magnetization is similar to the results obtained by Jaccarino and Walker in FeF_2 and CoF_2.[23]

MAGNETIC SUSCEPTIBILITY OF $Ni(IO_3)_2\cdot 2H_2O$

In an attempt to confirm our finding of the antiferromagnetic behavior of $Ni(IO_3)_2\cdot 2H_2O$ at low temperatures, a measurement of the susceptibility χ was undertaken.

χ_{rf}. Since neither rf nor dc measurements of χ existed, and because of the immediate availability of a suitable rf apparatus,[24] χ_{rf} was first determined. The sample was inserted into the resonant coil of a low-frequency (60 kc/sec) oscillator. The change in frequency of the oscillator, at a given temperature, when the sample was removed from the resonant coil was utilized in determining the inductance change in the circuit ($\delta\nu/\nu=\frac{1}{2}\delta L/L$). No attempt was made to calibrate our apparatus and therefore our procedure yields only the relative magnitude of χ_{rf} as a function of

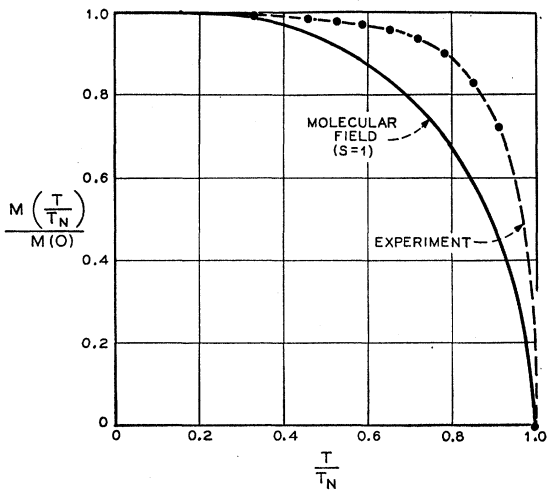

FIG. 4. The normalized temperature dependence of the internal magnetic field at the I^{127} nucleus in the antiferromagnetic state of $Ni(IO_3)_2\cdot 2H_2O$ as a function of the reduced temperature (T/T_n). This field is taken to be proportional to the sublattice magnetization and is indicated by the dashed line. In addition, the molecular field calculation for the spontaneous magnetization for $S=1$ is given by the solid line.

[23] V. Jaccarino and L. R. Walker, Phys. Rev. (to be submitted).
[24] A. L. Schawlow and G. E. Devlin, Phys. Rev. **113**, 120 (1959).

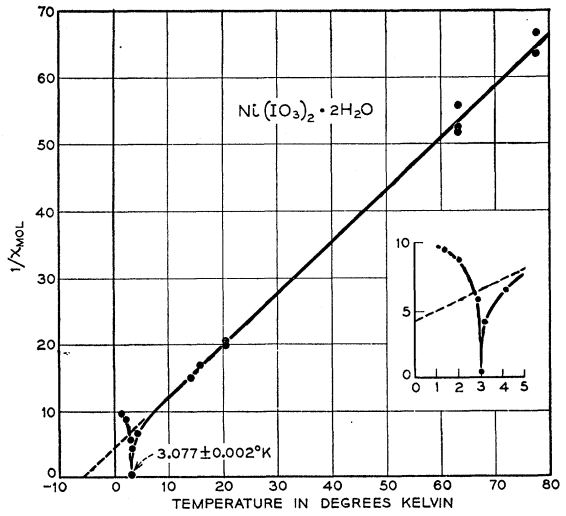

FIG. 5. The reciprocal of the molar susceptibility (at 60 kc/sec) $1/\chi_{mol}$, of $Ni(IO_3)_2 \cdot 2H_2O$ as a function of temperature. Absolute values of $1/\chi_{mol}$ were obtained using the calculated Curie constant for the Ni^{++} ion and assuming a Curie-Weiss behavior for $T \gg T_n$.

temperature. The absolute value of χ was obtained by assuming a Curie-Weiss behavior at high temperatures and using the calculated Curie constant for Ni^{2+}.

Figure 5 gives the results of these measurements showing the temperature dependence of the reciprocal molar susceptibility as a function of temperature. The unusual behavior of $1/\chi$ at 3.08°K was not expected. The reciprocal susceptibility has fallen far below the value for a paramagnet (given by the dashed line). This indicates the presence of a spontaneous rf ferromagnetic moment, the onset of which coincides with our NQR determination of T_n. The antiferromagnet NiF_2 is known to have a small ferromagnetic moment below T_n from the work of Stout.[25] Figure 6 gives the results of an independent rf susceptibility measurement we have made using powdered NiF_2. The absolute values in this figure were

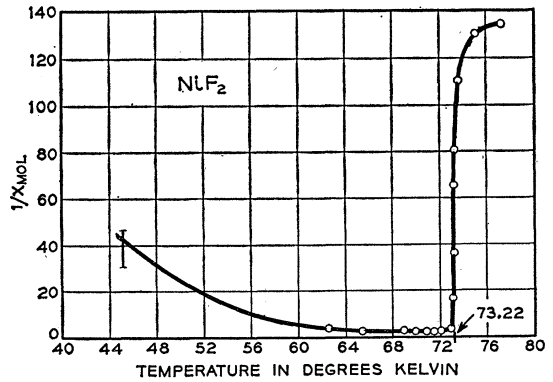

FIG. 6. The reciprocal of the molar susceptibility (at 60 kc/sec) $1/\chi_{mol}$, of NiF_2. Absolute values were obtained using the dc measurements of DeHaas *et al.*[26]

[25] L. M. Mataresse and J. W. Stout, Phys. Rev. **94**, 1792 (1954).

obtained by use of a measurement at 77.9°K by DeHaas *et al.*[26] It is interesting to note that while the rf moment in NiF_2 tends to persist well below T_n, the rf moment of $Ni(IO_3)_2 \cdot 2H_2O$ disappears almost immediately below T_n. For antiferromagnetic crystals satisfying certain crystal symmetry properties, a cocking of the sublattice magnetization resulting in a small ferromagnetic moment is not unexpected.[27,28]

The value 3.077°±0.003°K obtained from Fig. 5 agrees well with 3.08°K determined from the NQR. Extrapolation of the linear portion of the $1/\chi_{rf}$ curve yields a Curie-Weiss temperature θ, of approximately −5°K.

χ_{dc}. Some months after the results of χ_{rf} were obtained, Williams and Sherwood[29] measured the dc susceptibility χ_{dc}, in the temperature range 1.4°K to 60°K. Their results are given in Fig. 7 and generally confirm the rf measurements with one noticeable exception. The spontaneous ferromagnetic magnetization

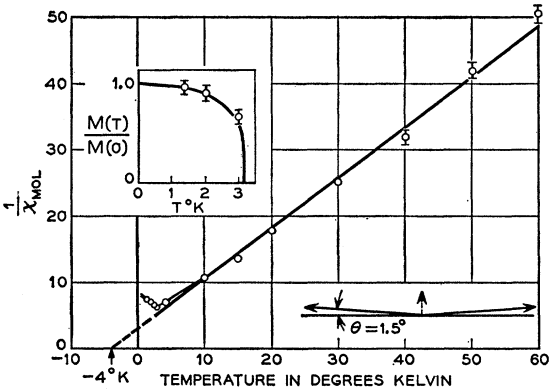

FIG. 7. The reciprocal of the dc susceptibility $1/\chi_{mol}$ of $Ni(IO_3)_2 \cdot 2H_2O$ versus temperature as measured by Williams and Sherwood. The insert in the upper left-hand corner of the figure is the spontaneous *ferromagnetic* moment observed below T_n, normalized to its extrapolated $T=0$ value, plotted versus T. In the lower right-hand corner is a schematic indication of the cocking of the two sublattices that results in a net ferromagnetic moment. The angle given is that which is determined from experiment.

that develops below T_n increases monotonically with decreasing temperature as is indicated in the insert of the same figure. A diagrammatic representation of the cocking of the antiferromagnetic sublattice magnetizations resulting in a net ferromagnetic moment is given in the lower right-hand corner of Fig. 7. As would be expected, the ferromagnetic moment would have the same temperature dependence as the antiferromagnetic sublattice magnetization.

The magnetization per gram of the spontaneous ferromagnetic moment, extrapolated to $T=0$, is 1.45 emu/g.

[26] W. J. DeHaas, B. H. Schultz, and J. Koolhoos, Physica **7**, 57 (1940).
[27] I. E. Dzialoshinskii, J. Exptl. Theoret. Phys. (U.S.S.R.) **33**, 1454 (1957) [translation: Soviet Phys.-JETP **6**(33), 1120 (1957)].
[28] T. Moriya, Phys. Rev. **117**, 635 (1960).
[29] H. J. Williams and R. C. Sherwood (unpublished).

If we assume the magnetization of Ni^{2+} to be saturated at $T=0$, we may calculate its magnitude

$$M_{\text{gram}}=N_{\text{gram}}g\beta S=27.2 \text{ emu/g}. \quad (5)$$

From this we obtain a cocking angle of 1.5°.

The sudden decrease in χ_{rf} as T drops below T_n is presumably associated with the decrease in domain wall motion resulting from a large anisotropy energy which spatially restricts the motion of the Ni^{2+} spins. Such a result is not surprising since the anisotropy energy of the Ni^{2+} spin in an electrostatic field of less than cubic symmetry is of the order of 2°–4°K. We thus have a case in which the effective anisotropy and exchange "fields" are comparable in magnitude. A detailed examination of the antiferromagnetic properties of NiF_2, where the local symmetry of the Ni^{2+} is known, has been made by Moriya.[28]

ISOTOPIC EFFECTS ON T_n FROM χ_{rf}

The extraordinarily abrupt increase (see Fig. 8) in the rf susceptibility as one approaches T_n, from either above or below in temperature, immediately suggests using χ_{rf} as a sensitive measure of any effect which might cause a variation in T_n (e.g., isotopic change, external pressure, etc.). Samples of isotopically enriched nickel iodate were prepared by Remeika. A change in T_n, relative to $Ni(IO_3)_2\cdot 2H_2O$ (natural isotopic abundance for all atoms), was searched for in $Ni(IO_3)_2\cdot 2D_2O$, $Ni^{58}(IO_3)_2\cdot 2H_2O$, and $Ni^{60}(IO_3)_2\cdot 2H_2O$. For the deuterated salt the change in T_n, if any, was less than 0.01°K and for the Ni^{58} and Ni^{60} salts an upper bound of 0.04°K was obtained. (The relatively larger uncertainty in the latter two samples results from increased experimental error associated with the small quantities that were prepared in these two cases.)

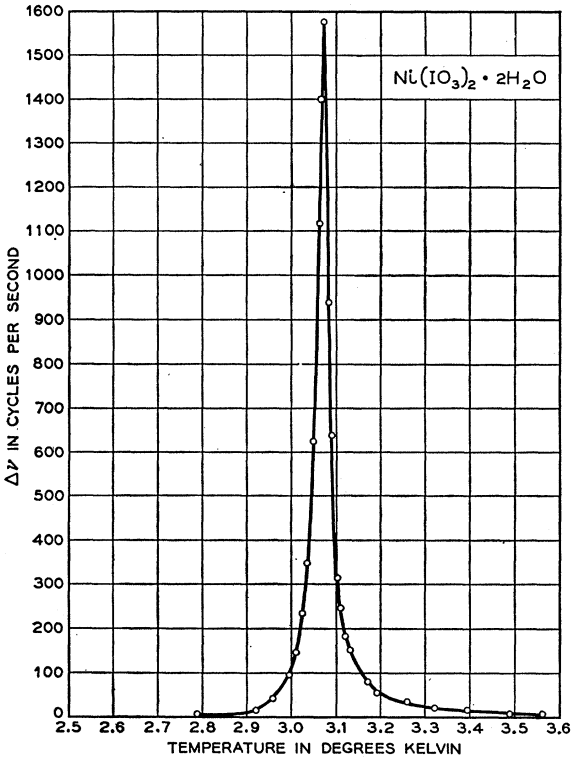

FIG. 8. The shift in frequency versus temperature for a sample of $Ni(IO_3)_2\cdot 2H_2O$ embedded in the resonant coil of a low-frequency oscillator (60 kc/sec). The unusually sharp peak in the frequency shift at T_n was utilized in investigating the effects on T_n due to isotopic variation.

ACKNOWLEDGMENTS

We wish to thank Mr. J. P. Remeika for preparing the enriched isotope samples, Mrs. E. A. Wood for permission to quote from her work on the crystal structure of $Ni(IO_3)_2\cdot 2H_2O$ prior to publication, Mr. J. L. Davis for experimental assistance, Dr. T. Moriya for several discussions concerning the ferromagnetic moment of $Ni(IO_3)_2\cdot 2H_2O$, Dr. M. Peter for the use of his computer program, and Mr. C. E. Miller for suggestions on the preparation of the samples. We are indebted to H. J. Williams and R. C. Sherwood for the dc susceptibility measurements of $Ni(IO_3)_2\cdot 2H_2O$.

APPENDIX. NQR OF THE OTHER COMPOUNDS INVESTIGATED

$(\pm\frac{3}{2}\leftrightarrow\pm\frac{1}{2})$ transitions. Figure 9 and Table II give the NQR frequencies of $Br^{79}(I=\frac{3}{2})$ in the bromates (of which large single crystals were grown from a saturated solution by a procedure originally developed by

TABLE II. Summary of $(\pm\frac{3}{2}\rightarrow\pm\frac{1}{2})$ NQR frequencies (in Mc/sec) as a function of temperature for the cubic bromate-hexahydrates and copper and nickel iodates. Data at 290°, 285°, and 195°K taken from reference 17.

Temp(°K)	$Co(BrO_3)_2\cdot 6H_2O$	$Ni(BrO_3)_2\cdot 6H_2O$	$Cu(BrO_3)_2\cdot 6H_2O$	$Zn(BrO_3)_2\cdot 6H_2O$	$Ni(IO_3)_2\cdot 2H_2O$	$Cu(IO_3)_2\cdot 2H_2O$
290	176.92	177.62				
285			175.70	177.38		
195	179.10	179.51	177.48	179.49		
77.2	181.07±0.03	181.23±0.03		181.34±0.03		154.5
20.3	181.45±0.03	181.72±0.03	181.82±0.03	181.62±0.03	148.8±0.1	154.5
14.0		181.75±0.03	181.82±0.03		148.8±0.1	
4.2	181.56±0.03	181.75±0.03	181.82±0.03		148.97	
1.3	181.56±0.03	181.75±0.03	181.77±0.03		(see body of paper)	154.5

[30] A. N. Holden (private communication).

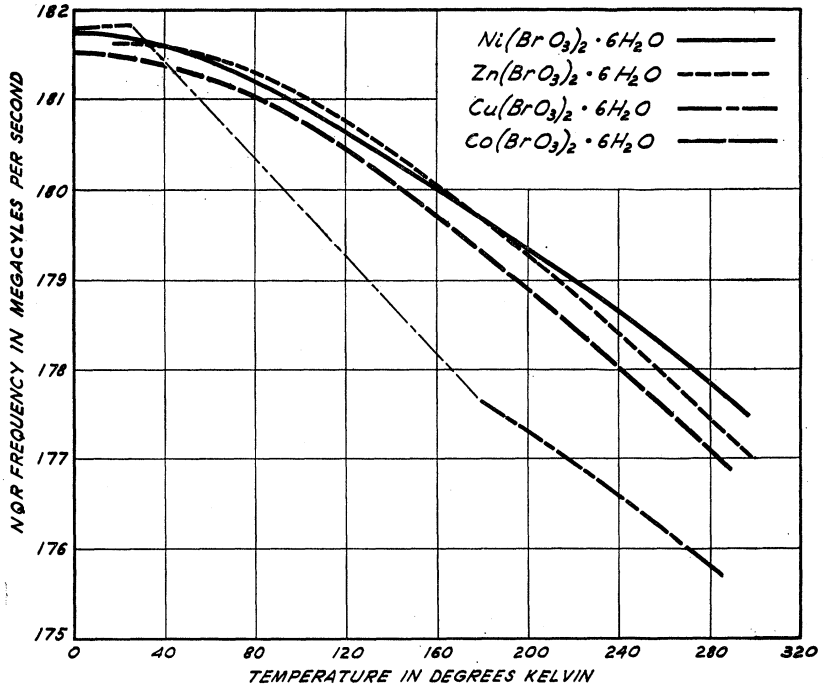

FIG. 9. The temperature dependence of the NQR frequency of the $Br^{79}(\pm\frac{3}{2} \leftrightarrow \pm\frac{1}{2})$ transitions in the four bromates (see Appendix I).

Holden[30]) and of I^{127} in nickel and copper iodate (the latter prepared in the same manner as the $Ni(IO_3)_2 \cdot 2H_2O$). The Br^{79} linewidths are all about 30 kc/sec. No concerted effort was made to find the second resonance in $Cu(IO_3)_2 \cdot 2H_2O$. The break in the curve for $Cu(BrO_3)_2 \cdot 6H_2O$ and the slight decrease of the NQR frequency at 1.3°K are most probably manifestations of the Jahn-Teller effect on the Cu^{2+} ion in a cubic environment.[31,14] Bayer's theory of the NQR temperature dependence[32] may be fitted by assuming a torsional vibration frequency for the BrO_3^- ion of $\omega \sim 2 \times 10^{13}$ sec^{-1} in the other three bromates.

$(\pm\frac{1}{2} \leftrightarrow \mp\frac{1}{2})$ *transitions.* For a single crystal in a uniform magnetic field, a resonance between the $m=+\frac{1}{2}$ and $m=-\frac{1}{2}$ quadrupole levels is observable. Although no extensive measurements were made, it was verified using $Co(BrO_3)_2 \cdot 6H_2O$ that the Z axis of the electric field gradient tensor in the bromates is along the [111] direction as expected from crystal symmetry considerations. The effective g value for the bromine nucleus in $Co(BrO_3)_2 \cdot 6H_2O$ along the [001] direction at 20°K is 1% higher than the accepted value. This is probably caused by the magnetic dipole field of the Co^{++} ions.[9]

[31] H. A. Jahn and E. Teller, Proc. Roy. Soc. (London) **A161**, 220 (1937).
[32] H. Bayer, Z. Physik **130**, 227 (1957).

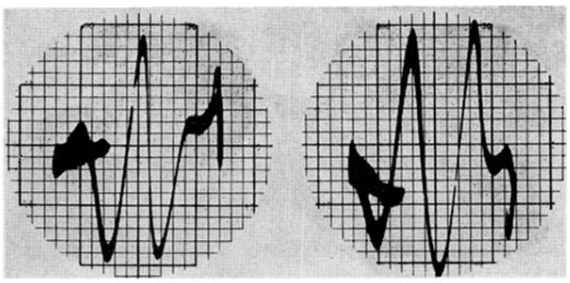

FIG. 3. Photograph of the oscilloscope presentation of the I^{127} NQR transition ($\pm\frac{5}{2} \leftrightarrow \pm\frac{3}{2}$) when (a) $T=4.2°K$ ($T>T_n$) and (b) $T=1.3°K$ ($T<T_n$). Calculations indicate that at 1.3°K all observed lines are actually doublets with a 536 kc/sec splitting. In order to resolve such doublets with a super-regenerative detector, one needs a quench frequency greater than the linewidth and either very much less or very much greater than the splitting. Because the lines are so broad in this case, one must use a quench frequency very much greater than 500 kc/sec. The detector used would not operate with such quench frequencies. The patterns on the oscilloscope were therefore not absorption lines but rather interference patterns of two lines and their images from sidebands of the detector. The frequencies used in the calculations were the frequencies of the centers of symmetry of the patterns. As would be expected, changing the quench frequency changed the pattern but did not shift its center of symmetry.